



ANALYSIS OF THE STRUCTURE OF VORTEX PLANAR FLOWS AND THEIR CHANGES WITH TIME

A.M. Filimonova, V.N. Govorukhin

Southern Federal University, Rostov-on-Don, Russian Federation

A numerical approach is proposed for studying changes in the structures of vortex configurations of an ideal fluid with time. Numerical algorithms are based on the solution of the initial-boundary value problem for nonstationary Euler equations in terms of vorticity and stream function. For this purpose, the spectral meshless vortex method is used. It is based on the approximation of the stream function by the Fourier series cut and the approximation of the vorticity field by the least squares method from its values in marker particles. To calculate the dynamics of particles, a Cauchy problem is solved. The scheme of the spectral-vortex method makes it possible to implement the algorithm for analyzing the “instantaneous structure” of the velocity field using the methods of the theory of dynamic systems. This includes the construction of an “instantaneous” vector flow field, its singular points, and saddle point separatrices. To study the dynamics of changes in structures with time, the field of the local Lyapunov exponents is calculated. The results of numerical modeling and the analysis of changes in the structure of vortex flows are presented on the basis of the proposed approaches for two types of boundary conditions. Under periodic boundary conditions, the vortex configuration consists of four vortex spots. For the flow condition, the fluid flow in the channel with a given velocity at the boundary is considered. The calculations have shown the effectiveness of the proposed algorithms for a fine analysis of the emerging pattern of the velocity field of the vortex configuration.

Key words: hysteresis and bifurcations, thermal density inversion, constant heat flux, finite difference method

1. Introduction

The analysis of vortex dynamics is important for understanding many natural processes and their dependence on the environment characteristics. Methods of bifurcation theory are effective for qualitative investigation of the influence of various parameters on the vortex structures dynamics and forming [1, 2]. Complex flows of an inviscid incompressible fluid consist of vortices with different intensity, size, and orientation. Their disposition at each moment of time determines the amount of mass transfer, the fluid dynamics, and the trajectories of the particles [3]. The information obtained about vortex dynamics in a fluid flow is relevant both for understanding the fundamental laws of fluid flow and for solving specific problems (see article [4] and literature review therein). The transformation of the flow structure in time and space leads to qualitative changes in the flow properties. Understanding the details of flow’s internal configuration makes it possible to study the interaction processes of vortex spots [5], evaluate and predict mass transfer in them [6]. It is possible by using numerical methods based on the theory of dynamical systems [7] and including both methods of the qualitative theory of differential equations and algorithms for the analysis of chaotic dynamics. In this article, an algorithm for the complex analysis of the structures of plane flows of an inviscid incompressible fluid is proposed. This algorithm is based on the spectral-vortex mesh-free method for solving a non-stationary problem for the Euler equations [8, 9].

2. Mathematical formulation of the problem and spectral vortex method

Plane flows of an inviscid incompressible fluid are considered. The problem can be described by the Euler equations, which in terms of vorticity $\omega(x, y, t)$ and stream function $\psi(x, y, t)$ have the form:

$$\begin{cases} \omega_t + \psi_y \omega_x - \psi_x \omega_y = 0, \\ -\Delta \psi = \omega, \end{cases} \quad \begin{matrix} 1 \\ 2 \end{matrix} \quad (1)$$

where t is the time, x, y are spatial coordinates, $\Delta \psi \equiv \psi_{xx} + \psi_{yy}$ is the Laplace operator. The equation (1)₁ describes the passive vorticity transfer by fluid particles. The equation (1)₂ relates the vorticity ω and the stream function ψ . The dimension of the quantities is omitted here and below. This is due to the fact that the Euler equations written for an inviscid incompressible fluid are dimensionless.

Two-dimensional flows in a rectangular area of the size $a \times b$ are investigated:

$$D = \left\{ (x, y) : -\frac{a}{2} \leq x \leq \frac{a}{2}; -\frac{b}{2} \leq y \leq \frac{b}{2} \right\}$$

with an initial condition $\omega(x, y, 0) = \omega_0(x, y)$. The problem is solved under two types of boundary conditions.

I. Space-periodic conditions

Under such conditions, restrictions arise for the initial condition, namely the integral over the domain D of $\omega_0(x, y)$ must be equal to zero. These boundary conditions are often applied in numerical modeling of vortex dynamics on the entire plane:

$$\psi \Big|_{-\frac{a}{2}} = \psi \Big|_{\frac{a}{2}}, \quad \psi \Big|_{-\frac{b}{2}} = \psi \Big|_{\frac{b}{2}}; \quad \psi_x \Big|_{-\frac{a}{2}} = \psi_x \Big|_{\frac{a}{2}}, \quad \psi_y \Big|_{-\frac{b}{2}} = \psi_y \Big|_{\frac{b}{2}}.$$

II. Given flow velocity at the boundary

In this case, it is assumed that the fluid flows through the boundary of the domain D with a given normal velocity. All the border of the domain D is divided into three parts: ∂D^+ , where the normal velocity of the fluid is directed into the area D (this corresponds to the entrance to the area); ∂D^- , where the normal velocity of the fluid is directed from the area D ; ∂D^0 , where is the solid boundary. Under such conditions, the flow velocity at the boundary of the region ∂D will be defined as:

$$\psi \Big|_{\partial D} = \psi^{\partial D},$$

where $\psi^{\partial D}$ is a given function satisfying the condition that the total fluid flow through the boundary is equal to zero. In addition, a boundary condition must be given for $\omega^+(x, y, t)$ at the entrance to the area (on part of the domain border ∂D^+).

To solve the non-stationary problem (1) means to find the characteristics of the behavior of vortex flows in time. For this, the spectral vortex method is used. It is based on the passive transfer of vorticity by marker particles and the representation of the stream function as a segment of the Fourier series. A detailed description of the numerical scheme of the method is presented in the works [8–10].

For both types of boundary conditions, the stream function ψ is approximated in the form of a segment of the Fourier series by the basis functions:

$$\psi(t, x, y) \approx \sum_{i=1}^{k_x} \sum_{j=1}^{k_y} \psi_{ij}(t) g_i(x) h_j(y). \quad (2)$$

Here: k_x, k_y are the number of expansion terms in x and y respectively; $\psi_{ij}(t)$ are unknown coefficients (they depend on the time t). The choice of functions $g_i(x), h_j(y)$ is determined by the type of boundary conditions:

– for the space-periodic boundary conditions

$$g_i(x) : \left\{ \frac{1}{\sqrt{a}}, \frac{\sqrt{2}}{\sqrt{a}} \sin\left(\frac{2\pi k}{a}\left(x + \frac{a}{2}\right)\right), \frac{\sqrt{2}}{\sqrt{a}} \cos\left(\frac{2\pi k}{a}\left(x + \frac{a}{2}\right)\right) \right\}, \quad k = 1, \dots, k_x,$$

$$h_j(y) : \left\{ \frac{1}{\sqrt{b}}, \frac{\sqrt{2}}{\sqrt{b}} \sin\left(\frac{2\pi k}{b}\left(y + \frac{b}{2}\right)\right), \frac{\sqrt{2}}{\sqrt{b}} \cos\left(\frac{2\pi k}{b}\left(y + \frac{b}{2}\right)\right) \right\}, \quad k = 1, \dots, k_y;$$

– for the condition with the given flow velocity at the boundary

$$g_i(x) : \left\{ \frac{\sqrt{2}}{\sqrt{a}} \sin \left(\frac{2\pi k}{a} \left(x + \frac{a}{2} \right) \right) \right\}, \quad k = 1, \dots, k_x,$$

$$h_j(y) : \left\{ \frac{\sqrt{2}}{\sqrt{b}} \sin \left(\frac{2\pi k}{b} \left(y + \frac{b}{2} \right) \right) \right\}, \quad k = 1, \dots, k_y.$$

Coefficients $\psi_{ij}(t)$ of the series (2) are calculated by solving the equation (1)₂ at each moment in time by the Bubnov-Galerkin projection method. After that, the dynamics of the marker particles of the fluid is described by a system of ordinary differential equations:

$$\begin{aligned} \dot{x}_i = v_x = \psi_y(t, x_i, y_i) &= \sum_{k=1}^{k_x} \sum_{l=1}^{k_y} \psi_{kl}(t) g_k(x_i) \frac{\partial h_l(y_i)}{\partial y}, \\ \dot{y}_i = v_y = -\psi_x(t, x_i, y_i) &= - \sum_{k=1}^{k_x} \sum_{l=1}^{k_y} \psi_{kl}(t) \frac{\partial g_k(x_i)}{\partial x} h_l(y_i), \end{aligned} \quad (i = 1, \dots, N). \quad (3)$$

In (3) (x_i, y_i) are spatial coordinates of the marker particles.

To solve the system (3), it is necessary to determine the initial coordinates of the particles (x_i^0, y_i^0) , and the corresponding vorticity value according to the initial condition $\omega_i = \omega_0(x_i, y_i)$. It is important that the coordinates of the particles change in time, but the vorticity values ω_i remain constant. Some of the marker particles are located in the nodes of a uniform grid. The coordinates of these nodes are used further for calculating the field of local Lyapunov exponents (LLE). The remaining particles can be distributed randomly. To detail the vorticity distribution of some subdomains, for each particle with coordinates (x_i^0, y_i^0) must be specified the particles that are symmetrical with respect to the axes $x=0$ и $y=0$. It is necessary in order not to disturb the discrete symmetries in the computational domain.

In the article [11], the method of solving the non-stationary problem is expanded due to algorithms for analyzing the structure and rearrangements of vortex structures in time in a closed flow domain. This article supplements the analysis of the problems of two-dimensional dynamics of an inviscid incompressible fluid under various boundary conditions with new possibilities.

In the calculations, the number of marker particles are from 20,000 to 160,000. That is, systems from 40,000 to 3,200,000 ordinary differential equations were numerically solved. This required parallelization of the algorithm for solving problem (3) using OpenMP technology. To integrate the system (3), a pseudo-symplectic integrator of the third order of accuracy and the sixth order of approximation of the symplecticity condition was used [12].

3. Algorithms for numerical analysis of vortex structure dynamics

It is known [3] that the "frame" of a complex plane flow is vortex spots, which determine the structure of the flow and the properties of fluid transfer. At each fixed moment of time in the center of the vortex spot, the velocity of the liquid is equal to zero, that is, the elliptical singular point of the system (3) corresponds to the center of the spot. In this case, the boundaries of the vortex spots are determined by separatrices, which are stable and unstable manifolds of saddle singular points of the system. The representation of the current function in the form (2) makes it possible to apply the approaches of the theory of dynamical systems to study the transformations of flows based on the rearrangements of the phase portraits of the system (3). In this paper, we propose an algorithm for automatic constructing a phase portrait at the values of the coefficients given in (3). Its description is given below.

The disadvantage of this approach is that a "momentary" structure of the velocity field is obtained, according to which it is possible to analyze fluid configurations only at a fixed time moment. At the same time, the flow structure is well represented only in the stationary case, and there is no idea about the details of dynamic rearrangements and mass transfer processes in non-stationary fluid flows.

Information about unsteady vortex flows can be obtained by studying the nature of marker particles trajectories in time. The chaotic character of the trajectories will indicate the dependence of the flow velocity field on time. When a liquid particle moves in space, it passes through regions with different dynamics, and the motion of the

particle can be characterized by the magnitude of its acceleration [12], which makes it possible to study the processes of fluid transfer. The algorithm for calculating particle trajectories is an integral part of the scheme of the spectral vortex method, the description of which can be found in the articles [8-10].

The intensity and structure of mass transfer can be obtained as a result of calculating the LLE field. This characteristic is constructed without significant additional effort when using the spectral vortex method. The calculations involve particles located in the nodes of a rectangular grid in the flow region (see [9, 11]).

3.1. Algorithm for constructing the "instant structure" of the velocity field

Stage I of the algorithm for numerical analysis of the vortex structure dynamics of the flow consists in finding all the singular points of the velocity vector field of fluid particles. To do this, a system of two algebraic equations of the form is solved:

$$\begin{aligned}\psi_y(x, y) &\approx \sum_{k=1}^{k_x} \sum_{l=1}^{k_y} \psi_{kl} g_k(x) \frac{\partial h_l(y)}{\partial y} = 0, \\ \psi_x(x, y) &\approx \sum_{k=1}^{k_x} \sum_{l=1}^{k_y} \psi_{kl} \frac{\partial g_k(x)}{\partial y} h_l(y) = 0.\end{aligned}\tag{4}$$

To obtain a solution, it is natural to use Newton's method.

Let us introduce the notation: $F = (\psi_y(x, y), -\psi_x(x, y))$ and $U = (x, y)$. The calculation formula of the method will take the form: $U^{k+1} = U^k - J^{-1}(U^k) \cdot F(U^k)$, where J is the Jakobi matrix of the system (4).

With a well-defined initial approximation, Newton's method will converge to one of the solutions. Finding all solutions of the system (4) is a much more complex problem, which is generally difficult to solve.

To search for the set of singular points of the system (4), the following sequence of actions can be proposed:

1. The calculation domain D is divided into cells with step h .
2. As an initial approximation for the Newton method, the coordinates of the cell center are selected.
3. Next, perform calculations according to the Newton method. For a cell, the iterative process is completed in one of two cases: the next value has gone beyond the boundaries of the cell; the equilibrium value — U_* , is found.
4. The obtained solutions should be analyzed for stability and classified into singular points (saddle and elliptical).

Steps 1-4 of the algorithm are performed with step $h/2$.

5. If the number of solutions found are the same, stop the algorithm.

Stage II of the algorithm consists in constructing stable and unstable manifolds U_* and saddle points. These special trajectories will be the separatrices of vortex spots. It is necessary to find eigenvectors corresponding to positive (u) and negative (v) eigenvalues U_* for each saddle point. Then we need to solve system (3) in forward time $t \in [0, T]$ with the initial condition $U_* \pm \delta u$ and in reverse time $t \in [-T, 0]$ with the initial condition $U_* \pm \delta v$. The value T is determined in the calculation process. The calculation stops either when the trajectory hits the boundary of the flow region in the vicinity of another singular point, or when the time reaches a certain maximum value T_{\max} .

3.2. Construction of a field of the local Lyapunov exponents (LLE)

The Lyapunov exponents help to analyze mixing and mass transfer processes in a fluid qualitatively. They also allow detecting stagnant zones. Using the Lyapunov exponents makes it possible to determine how infinitely close at the initial moment liquid particles move away from each other over the time. Since vortex structures are studied at finite times, we are talking about LLE field. In this paper, LLE calculation is based on the schemes described in [14, 15]. This approach is in good agreement with the algorithm of the spectral vortex method [8, 11]. A distinctive feature of the applied approach is the consideration of the dynamics of marker particles in the entire domain, including particles with zero vorticity, which opens up the possibility of effortlessly constructing the LLE field at each time step.

When constructing the LLE field in the flow domain D , particles located in the nodes of a rectangular grid at a t_0 time moment are used. These particles determine the initial vorticity distribution in the domain D . Let (x_i^0, y_i^0) be the initial coordinates of the particle with the number i ($i=1, 2, \dots, N$) on the plane. Then $U(x_i^0, y_i^0, T) = (x_i^0(t_0 + T), y_i^0(t_0 + T))$ are the coordinates of the i -particle at the T time moment, where t_0 is the initial moment of time. The local Lyapunov exponent at T time is defined as follows:

$$\sigma^T(x_i^0, y_i^0) = \frac{1}{|T|} \cdot \ln \sqrt{\lambda_{\max}^i \left((\nabla U)^T \cdot \nabla U \right)}, \tag{5}$$

where λ_{\max}^i — is the maximum eigenvalue of the Cauchy–Green strain tensor $\left((\nabla U)^T \cdot \nabla U \right)$ for the particle (x_i^0, y_i^0) .

The value $\nabla U(x_i^0, y_i^0)$ in expression (5) is calculated by using a four-point pattern. For the convenience of using this approximation scheme, we apply two-index numbering of particles: $x_{k,l}^0 = k \cdot h_x$, $y_{k,l}^0 = l \cdot h_y$, where $k = 1, \dots, m_x$, $l = 1, \dots, m_y$. Here h_x , h_y are fragmentation steps by x and y respectively, m_x , m_y — are the number of grid nodes b on axes x and y respectively. Then the formula for the calculation $\nabla U(x_{k,l}^0, y_{k,l}^0)$ will take the form:

$$\nabla U(x_{k,l}^0, y_{k,l}^0, T) \approx \left[\frac{\nabla U(x_{k+1,l}^0, y_{k+1,l}^0) - \nabla U(x_{k-1,l}^0, y_{k-1,l}^0)}{2h_x}, \frac{\nabla U(x_{k,l+1}^0, y_{k,l+1}^0) - \nabla U(x_{k,l-1}^0, y_{k,l-1}^0)}{2h_y} \right]. \tag{6}$$

Since all values in the right part of expression (6) are known at each time step T , to construct the LLE field at the nodes of a rectangular grid, it is necessary to calculate the value $\nabla U(x_{k,l}^0, y_{k,l}^0)$ according to formula (6) for each node of the grid and find the maximum eigenvalue of the strain tensor. The maximum eigenvalue λ_{\max} can easily be calculated analytically. After that, the LLE value is found according to the formula (5).

4. Verification of the Method

The proposed numerical scheme has been verified by a number of test calculations. For periodic boundary conditions, the dynamics of the Lamb dipole was studied, given at the initial time by the following vorticity distribution:

$$\omega_0(x, y) = \begin{cases} \frac{2\lambda U}{J_0(\lambda R)} J_1(\lambda r) \cos \Theta, & r \leq R, \\ 0, & r > R, \end{cases} \tag{7}$$

where r , Θ are polar coordinates on the plane, J_i is Bessel functions of the 1st kind of i order (for the smoothness of the vorticity field we assume $\lambda R = 3.831$ is zero of the Bessel function of the 1st kind), $R = 0.5$ is Dipole’s radius, $U = 0.3$ is Dipole’s velocity.

Figure 1 shows lines of the stream function of the Lamb dipole (7) at the initial and final time moments of the calculation. During the calculation period, the dipole passed through the boundaries of the region ten times along the abscissa axis. It can be noted that the vortex configuration has completely retained its structure and symmetry, which allows us to conclude that the accuracy of calculations based on the proposed numerical scheme is quite high. The test calculation was carried out on the time interval $t \in [0, 350]$. The calculation parameters were: $a = b = 10$, $\Delta t = 0.015$ is time step, $k_x = k_y = 35$ are the number of expansion terms in x and y respectively, $n_x = n_y = 50$ are the number of domain D fragmentation by x and y respectively.

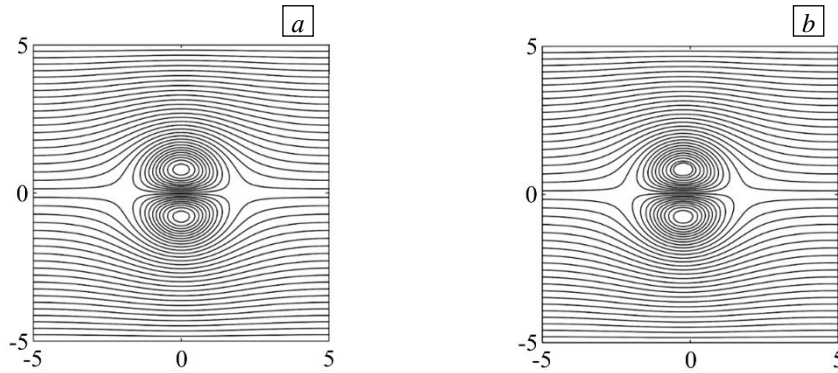


Fig. 1. Stream lines of the Lamb Dipole at the initial and final times $t : 0$ (a); 350 (b).

5. Numerical experiments

Two initial configurations were analyzed using the proposed algorithms. The algorithm of analysis is used in the first case of the "instantaneous structure" of the velocity field, and in the second of the constructed LLE field.

5.1. Analysis of the flow structure in the channel

This computational experiment demonstrates the possibilities and results of calculating the "instantaneous structure" of the flow velocity field. The flow in the channel with the sides $a = 3, b = 1$ is considered. Boundary conditions are of the type II with a given velocity of the flow on the boundary is a function in the form $\psi^{oD} = Q_1 y + Q_2 y^2 + Q_3 y^3$ and vorticity at the entrance to the channel is $\omega^+ = k\psi^{oD}$. Under such conditions, stationary modes are known in problem (1) with the dependence $\omega(x, y) = k\psi(x, y)$, (see [15]). As an initial configuration (initial distribution $\omega_0(x, y)$) let us choose a vortex configuration corresponding to the stationary mode at $Q_1 = 0.03, Q_2 = 0.21, Q_3 = -0.14, k = 51$. To implement the spectral vortex method, we use the following parameters: $N = 22000$ is quantity of particles; $n_x \times n_y = 30 \times 10$ is the number of cells in the partition of the domain D ; $k_x \times k_y = 35 \times 35$ is the number of expansion terms in (2); $h = 0.02$ is the time step. The results of the calculations are shown in Figure 2.

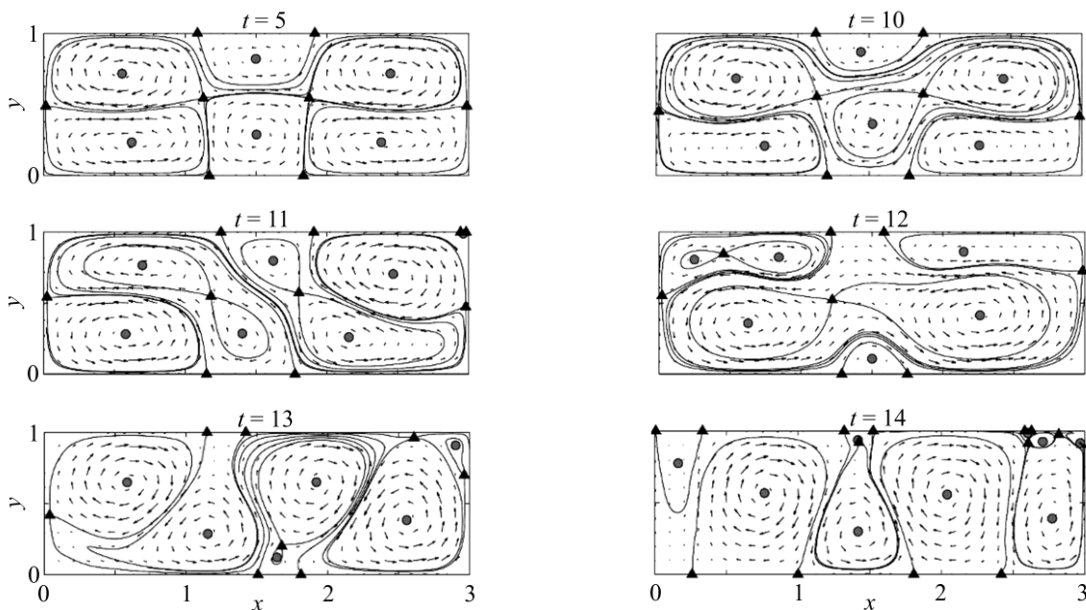


Fig. 2. The velocity field of the fluid in the channel at various points in time t ; saddle singular points are marked with a triangle; elliptical singular points are marked with a circle; separatrix of saddle points correspond to the lines.

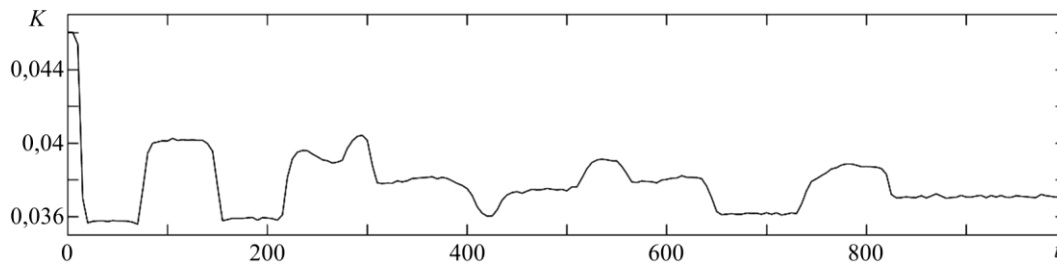


Fig. 3. Dependence of the kinetic energy K of the flow on time t .

At the initial time, the stationary mode is maintained, the velocity field at $t = 5$ contains 8 saddle and 6 elliptical singular points. At $t \approx 10$, the accumulated computational error leads to the destruction of the configuration of the stationary mode, the restructuring of the structure of the phase portrait (the reconnection of separatrices). On the time $t \in [10, 14]$, the flow undergoes a significant transformation: over time, the number of singular points, the nature of the separatrix, and the geometry of the flow zone change. At $t = 14$ the flow consists of five vortex spots that interact with growth, and the final flow mode is close to stationary, with a structure consisting of three vortices (not shown in the figure). Figure 3 shows a graph of the dynamics of the kinetic energy of the flow. Due to the openness of the channel, the energy changes over time, but in the final regime, which is close to stationary, these changes are small.

5.2. Dynamics of a system of four vortex patches

A vortex flow configuration consisting of four distributed vortex spots is considered. At the initial moment of time, the vorticity field is determined, according to the Gaussian law, as follows:

$$\omega_0(x, y) = \begin{cases} \frac{1}{\sqrt{2\pi}} e^{-\frac{(x \mp \alpha)^2 + (y \pm \beta)^2}{2}}, & (x \mp \alpha)^2 + (y \pm \beta)^2 \leq R^2, \\ -\frac{1}{\sqrt{2\pi}} e^{-\frac{(x \mp \alpha)^2 + (y \pm \beta)^2}{2}}, & (x \mp \alpha)^2 + (y \pm \beta)^2 \leq R^2, \\ 0, & (x \mp \alpha)^2 + (y \pm \beta)^2 > R^2, \\ 0, & (x \mp \alpha)^2 + (y \pm \beta)^2 > R^2, \end{cases} \quad (8)$$

where $(\pm\alpha, \pm\beta)$, $(\mp\alpha, \pm\beta)$ are coordinated of the centers of the vortex spots, R is the spot radius.

The dynamics of the vortex structure was studied under the following parameters: $a = b = 20$ are dimensions of the calculation domain D ; $N = 160000$ is the number of particles; $n_x \times n_y = 35 \times 35$ are the number of cells; $k_x \times k_y = 30 \times 30$ are the number of expansion terms in the Fourier series by x and y respectively; $\Delta t = 0.005$ is time step; $t \in [0, 1500]$ is the time period of calculation. The table shows the values of the parameters α , β , R , corresponding to the initial vortex configuration (8).

Table. Parameters of vortex configurations in a computational experiment.

Experiment number	α	β	R
I	5.0	5.0	4.5
II	4.0	4.0	2.0
III	5.0	5.0	3.5

The figures below show the results of computational experiments on modeling vortex flows on a plane. Figure 4 shows the initial distribution of vorticity and streamlines for each of the computational experiments. Black color means spots with negative vorticity value and while color means spots with positive vorticity value.

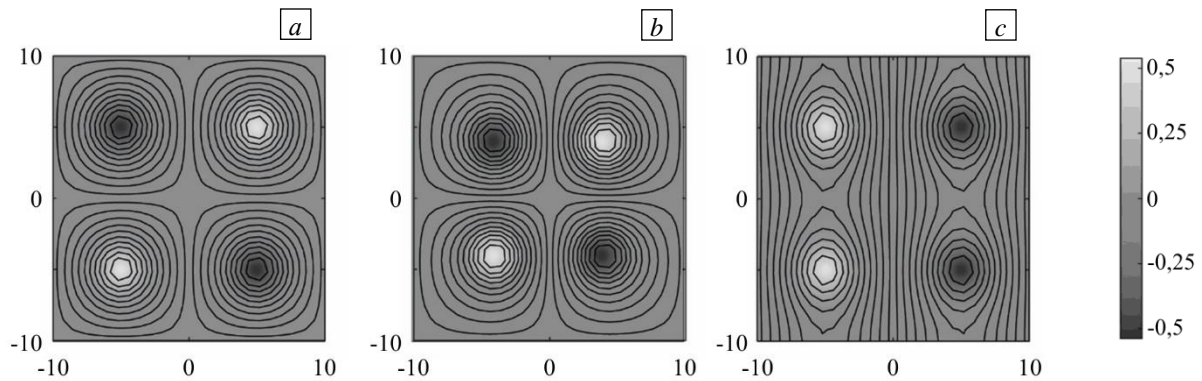


Fig. 4. Distribution of vorticity and stream function lines at the initial time $t = 0$ for experiments I (a), II (b), III (c).

Three different vortex configurations consisting of four distributed vortex spots of different signs are considered. At the initial moment of time, the vortex structures differ from each other in the coordinates of the spots centers, the radius of the spot, as well as the mutual location of the spots of different signs.

Figure 5 shows the final vorticity distribution and the type of streamlines for each of the experiments I–III. The vortex configuration in Figure 5a corresponds to a stable mode: the symmetrical flow structure remains unchanged during the entire calculation period. Each of the vortex spots rotates around its axis, remaining in place.

The dynamics of the vortex configuration II (see Fig. 5b) is a repetitive mode with a period $\tau \approx 180$. This means that the structure returns to its initial position during the time period τ . In total, during the experiment, it undergoes 8 complete cycles of change.

The vortex configuration III turned out to be unstable. During the calculation, it gradually changes and then completely collapses; a qualitatively new structure appears. Figure 5b shows that out of the four vortex spots characteristic of the initial moment of time, two larger vortex spots are formed. At the same time, the new vortex structure turns out to be more stable, unlike the configuration at the beginning of experiment III.

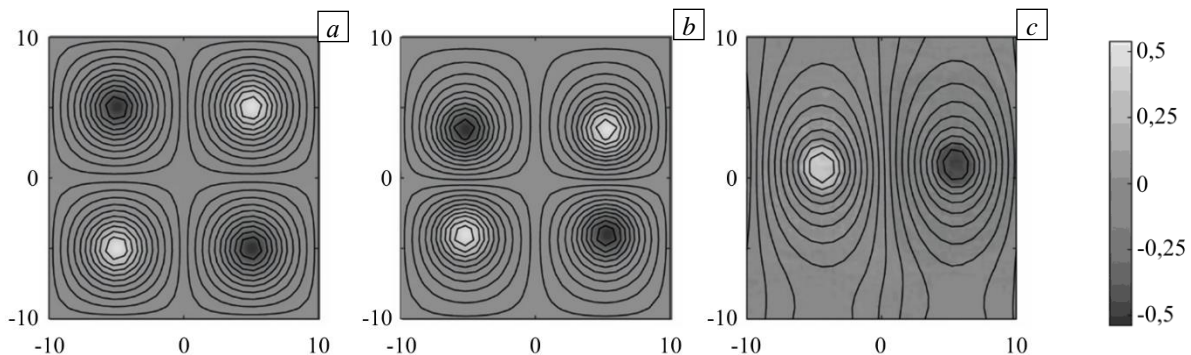


Fig. 5. Distribution of vorticity and stream function lines at the final time $t = 1500$ for experiments I–III, see respectively (a–c).

Figure 6 shows the LLE field for each of the experiments I–III at the finite time $t = 1500$. Here, black color means the smallest distance of the particles from each other over time (the minimum LLE is 0), and the lighter the shade of gray, the greater the value of the LLE and the greater the distance from each other the particles scatter. In Figure 6a there are two separatrices: vertical and horizontal. Mixing processes occur most intensively around rotating spots, which corresponds to the lightest shade of gray (Fig. 6b). The centers of each of the spots are in place during the entire estimated time. Particles close to the center of the spot scatter to a smaller distance than particles located near the contour of the spot. It is also possible to note the presence of two pronounced separatrices. Four stagnant zones are clearly visible, where the particles have practically not moved relative to each other.

In the image of the results of experiment III (see Fig. 6b), light gray color prevails. This means that there has been almost complete mixing in the area. The darkest areas here are the central points of the vortex spots: they remain in their places during the entire calculation time, while the surrounding particles move away from them

for quite long distances. In this figure, as well as in the images of the two previous experiments, a vertical separatrix is visible.

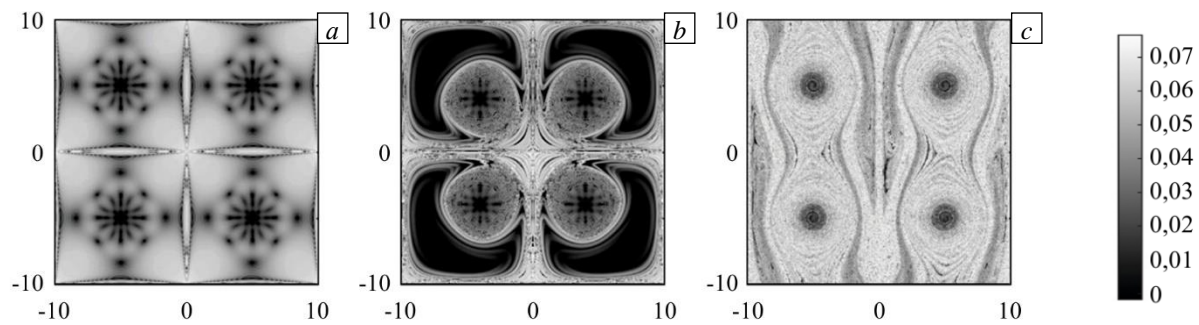


Fig. 6. LLE field at the final time for experiments I–III, see respectively (a–c).

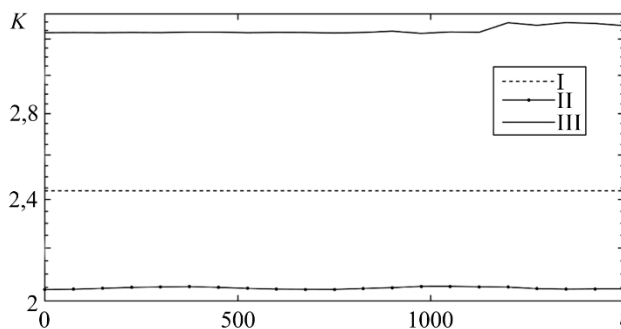


Fig. 7. Dependence of the kinetic energy K of the flow on time t for experiments I–III.

For a qualitative assessment of the results obtained at each moment of time on the step $t \in [0, 1500]$ in experiments I–III, the corresponding average value of kinetic energy was calculated by the formula $K = (v_1^2 + v_2^2) = \psi_x^2 + \psi_y^2$, where v_1, v_2 are the first and second components of the velocity vector v , ψ_x, ψ_y are the partial derivatives of the stream function ψ by variables x and y respectively. The results of the calculation are presented in figure 7. It can be seen that the value of the kinetic energy remains practically

unchanged over the entire time period of calculation.

For Experiment III, there is a slight increase in time moment $t \approx 1200$. This is due to the fact that it is at this time that a qualitative restructuring of the vortex structure takes place (two of the four vortex spots are formed). As a result of the merging of vortex spots, small-scale structures are formed, because of which the quality of the approximation of the vorticity field deteriorates. This leads to an increase in the error of the calculated values. The problem that arises can be eliminated by increasing the number of cells when constructing a discrete analogue of the domain.

6. Conclusion

The proposed algorithms for the qualitative analysis of the dynamics of vortex configurations based on the solution of the non-stationary problem of the dynamics of an inviscid incompressible fluid by the spectral-vortex mesh-free method make it possible to consider in detail the rearrangements of vortex configurations. The efficiency of the algorithms is confirmed by the calculations carried out. The resulting "instantaneous" phase portrait of the flow velocity field provides an opportunity to calculate the number and size of vortex spots at each moment in an acceptable time. The field of the local Lyapunov exponents allows one to estimate the intensity of fluid mixing in different flow zones over time.

The described approach can be used not only for solving direct problems of studying flows in time, but also for identifying a vortex configuration based on known data on the flow velocity field. A fairly simple implementation of the methods for qualitative analysis of the flow structure is due to the scheme of the spectral-vortex method for solving a non-stationary problem. The approximation of the current function by a segment of the Fourier series makes it possible to calculate the velocity vector at any point in the domain and use the methods of the theory of dynamical systems. However, when solving non-stationary problems using spatial discretization, for example, finite differences, the implementation of qualitative analysis algorithms is associated with additional difficulties.

The proposed algorithms were used to study the dynamics of various vortex configurations. In the case of a flow in the channel, the change in the structure of the vortex configuration and the velocity field over time is shown; all the singular points of the velocity field are found. The configuration of four distributed vortex spots on the plane was also investigated. The influence of the size of the spot radius and the relative position of co-

and multidirectional spots on the stability of the vortex configuration is considered. The evolution of the vortex structure over time is shown, the local Lyapunov exponents are calculated and estimated.

Acknowledgments. The study was carried out with financial support by RFBR (project № 19-29-06013).

References

1. Zhuravleva E.N., Puhnachev V.V. Numerical study of bifurcations in spiral fluid flow with free boundary. *Vychisl. mekh. splosh. sred – Computational Continuum Mechanics*, 2014, vol. 7, no. 1, pp. 82-90. <https://doi.org/https://doi.org/10.7242/1999-6691/2014.7.1.9>
2. Hasan M.S., Mondal R.N., Lorenzini G. Physics of bifurcation of the flow and heat transfer through a curved duct with natural and forced convection. *Chin. J. Phys.*, 2020, vol. 67, pp. 428-457. <https://doi.org/10.1016/j.cjph.2020.07.004>
3. Haller G. Lagrangian coherent structures. *Annu. Rev. Fluid Mech.*, 2015, vol. 47, pp. 137-162. <https://doi.org/10.1146/annurev-fluid-010313-141322>
4. Kolodezhnov V.N. Plane vortex flow in a cylindrical layer. *Vychisl. mekh. splosh. sred – Computational Continuum Mechanics*, 2021, vol. 14, no. 2, pp. 159-170. <https://doi.org/https://doi.org/10.7242/1999-6691/2021.14.2.13>
5. Cerretelli C., Williamson C.H.K. The physical mechanism for vortex merging. *J. Fluid Mech.*, 2003, vol. 475, pp. 41-77. <https://doi.org/10.1017/S0022112002002847>
6. Götzfried P., Emran M.S., Villermaux E., Schumacher J. Comparison of Lagrangian and Eulerian frames of passive scalar turbulent mixing. *Phys. Rev. Fluids*, 2019, vol. 4, 044607. <https://doi.org/10.1103/PhysRevFluids.4.044607>
7. Wiggins S. The dynamical systems approach to Lagrangian transport in oceanic flows. *Annu. Rev. Fluid Mech.*, 2005, vol. 37, pp. 295-328. <https://doi.org/10.1146/annurev.fluid.37.061903.175815>
8. Govorukhin V.N., Filimonova A.M. Numerical calculation of planar geophysical flows of an inviscid incompressible fluid by a meshfree-spectral method. *Komp'yuternyye issledovaniya i modelirovaniye – Computer Research and Modeling*, 2019, vol. 11, no. 3, pp. 413-426. <https://doi.org/10.20537/2076-7633-2019-11-3-413-426>
9. Govorukhin V.N. A vortex method for computing two-dimensional inviscid incompressible flows. *Comput. Math. and Math. Phys.*, 2011, vol. 51, pp. 1061-1073. <https://doi.org/10.1134/S096554251106008X>
10. Filimonova A.M. Dynamics and advection in a vortex parquet. *Izvestiya VUZ. Applied Nonlinear Dynamics*, 2019, vol. 27, no. 4, pp. 71-82. <https://doi.org/10.18500/0869-6632-2019-27-4-71-84>
11. Govorukhin V.N. Numerical analysis of the dynamics of distributed vortex configurations. *Comput. Math. and Math. Phys.*, 2016, vol. 56, pp. 1474-1487. <https://doi.org/10.1134/S0965542516080078>
12. Wang L. Analysis of the Lagrangian path structures in fluid turbulence. *Phys. Fluid.*, 2014, vol. 26, 045104. <https://doi.org/10.1063/1.4870702>
13. Shadden S.C., Lekien F., Marsden J.E. Definition and properties of Lagrangian coherent structures from finite-time Lyapunov exponents in two-dimensional aperiodic flows. *Phys. Nonlinear Phenom.*, 2005, vol. 212, pp. 271-304. <https://doi.org/10.1016/J.PHYSD.2005.10.007>
14. Haller G. Finding finite-time invariant manifolds in two-dimensional velocity fields. *Chaos*, 2000, vol. 10, pp. 99-108. <https://doi.org/10.1063/1.166479>
15. Govorukhin V.N. Steady vortex structures in inviscid flows in channels. *Fluid Dyn.*, 2012, vol. 47, pp. 147-156. <https://doi.org/10.1134/S0015462812020020>

The authors declare no conflict of interests.

The paper was submitted 02.07.2021; approved after reviewing 29.09.2021; accepted for publication 11.10.2021